Evaluating the IIF-1 for Aviation Users

R. Eric Phelts, Grace Xingxin Gao, Gabriel Wong, Liang Heng, Todd Walter, Per Enge,
Stanford University

Stefan Erker, Steffen Thoelert, *German Aerospace Center (DLR)*

The addition of any navigation satellite is significant to the GNSS community at a large, but the first Block IIF is perhaps especially important to the aviation community. While non-aviation users may take advantage of GNSS receivers that utilize any and all available ranging sources, aviation users must rely on signals that must meet strict criteria on performance and reliability. This often translates into demands for robust performance and high availability of service with fewer ranging sources upon which it can rely.

This is due to two primary reasons. For one, it requires that the navigation signals originate from trustworthy sources. GPS is one such source, of course. Although other satellite navigation systems exist or are anticipated in the future, these have either not yet arrived, or they simply have not gained the pedigree that GPS has earned from years of continued operation and dependable performance. The second reason is that signals used for safety of life Aeronautical Radionavigation Services (ARNS), must be in designated frequency bands to avoid interference from overlapping signals. GPS L1 is in a designated ARNS band, but L2 is not. However, the new L5 signal is also in an ARNS band, and, like L1, can be used for aviation.

Signals must also demonstrate that they meet the same performance as those in the legacy constellation. Because aviation users depend on these signals for safety of life operations, any new ranging sources must be monitored by the same systems that have guaranteed the integrity of existing constellation. For seamless integration into space-based and ground-based augmentation systems (SBAS and GBAS), this implies that any new signals must meet the same high standards that the existing signals have demonstrated.

SVN 62 and Signal Deformation Monitoring

For the new block IIF the question becomes: how do the new signals compare to the others? When significant differences between the transmitted chip shapes exist from satellite-to-satellite, these differences are referred to as signal deformations. They can lead to receiver range errors that vary as a function of receiver discriminator and filter characteristics. These in turn must either be corrected by the augmentation system, if possible, or must be modeled and accounted for in the error analyses. In extreme cases, an aberrant signal is flagged as unusable by an integrity monitor.

SBAS and GBAS currently employ signal deformation monitors to detect and exclude range sources that differ significantly from the other satellites. These systems make assumptions about the nominal deformations on the signals that have implications on system performance as well. Although non-aviation users can often leverage the fact that in-fact performance is usually a

blend of the worst-performing satellites and the best ones, augmentation system performance is frequently determined by the worst possible combination of range sources. This can often translate into a decrease in system availability and, hence, utility for all aviation users.

To evaluate the SVN 62 signals, we need to assure that it is compatible with the monitors. We would like to be certain that the existing assumptions that SBAS and GBAS make about the types of distortions, which hold for the existing constellation of GPS satellites, also apply for this satellite. More specifically, we desire that the code chips transmitted from SVN 62 have the same shape and duration as the others measured in the past. Further, we would like these properties to be independent of elevation angle. Note that this latter property was violated by a previous satellite and is important to establish prior to proceeding with more detailed analyses.

Elevation Angle Dependence

In early 2009, the navigation community got its first look at an L5 signal transmitted from a GPS satellite—SVN49. The Block IIRM satellite had been retrofitted with an L5 transponder to temporarily reserve spectrum for the upcoming Block IIF satellites. Unfortunately, that retrofit had the unintentional side-effect of introducing an internal reflection onto the L1 signal.

The details of this reflected signal have been studied and documented extensively by others, but the effect is significant to SBAS and GBAS. The transmitted signal is internally distorted by multipath. Worse yet, this distortion created errors that vary as a function of user receiver implementation and elevation angle. This latter effect can be particularly problematic for SBAS, since it protects the integrity of many different users observing the satellite over a wide range of elevation angles.

The following question naturally rises: "Does an elevation dependent bias also exist for SVN 62?" To answer this question, we processed the data from International GNSS Service (IGS) network to compare the elevation angle dependence of the two satellites. The same IGS site was used for both SVN 49 and SVN 62 in our study so that the receiver errors are comparable for each. The IGS site was selected based on the following requirements:

1. The receiver outputs measurements for both SVN 49 and SVN 62 satellites. As both satellites are set 'unhealthy' at this moment, many IGS sites do not output their measurements. All 300+ receivers in the IGS network were screened; only 69 of them provide data for both satellites as of Day 170, Year 2010.
2. The receiver observes both SVN 49 and SVN 62 at high elevation angles. As we evaluate the elevation dependency, we want the full (or near-full) span of the elevation. Figure 1 shows the ground tracks of the two satellites. We favored the receivers located in the vicinity of the cross point marked by a red circle.
3. The receiver noise is low. The two nearest receivers to the ground track cross point are 'brus' (Brussels, Belgium) and 'wsrt' (Westerbork, the Netherlands). We choose 'wsrt—a TurboRogue AOA SNR-12 receiver—for investigation. Although it is the second-nearest site, its receiver noise and multipath is lower than 'brus' based on our study. The longitude, latitude, and height of the site are +4.3592 degrees° (Longitude), +50.7978° (Latitude) and 149.7 m (above geoid) respectively.

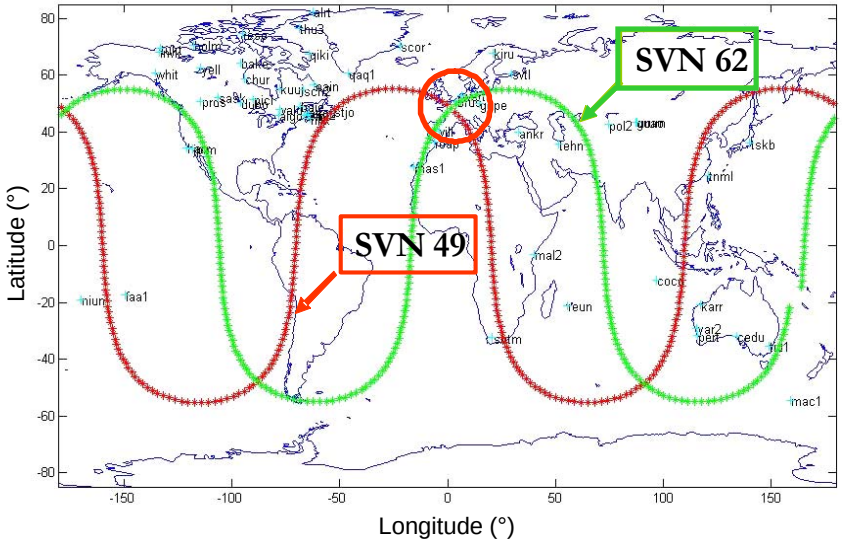

Figure 1. Ground tracks of SVN 49 and SVN 62. The receivers shown on this map are the 69 out of 300+ IGS sites that output both SVN 49 and SVN 62 measurements as of Day 170, Year 2010.

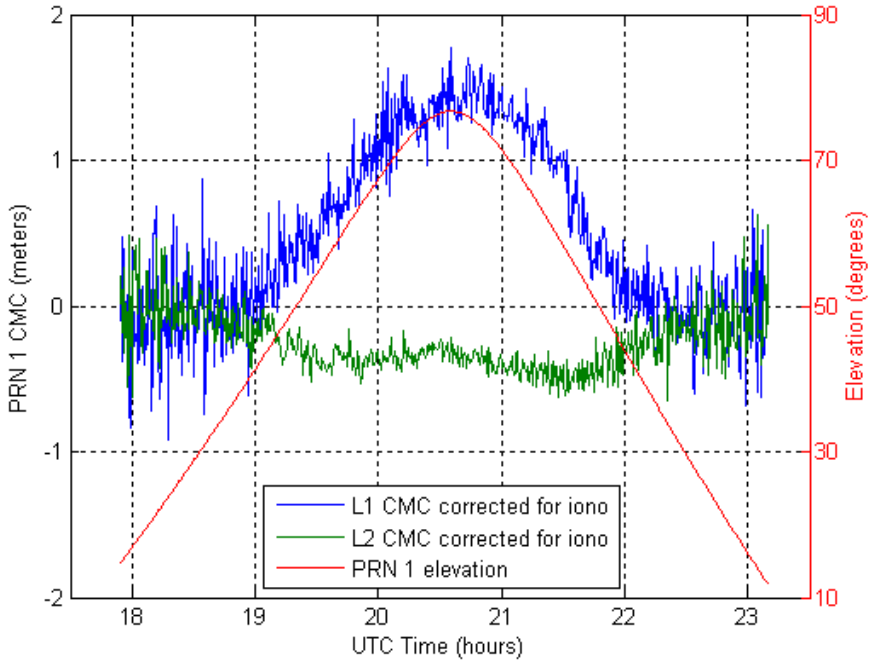

Figure 2. SVN 49 code-minus-carrier measurements after applying a dual-frequency ionosphere correction. The clock, orbit, troposphere, and ionosphere errors are all eliminated. An obvious positive elevation-dependent bias exists in the L1 C/A measurements. A slight negative elevation-dependent bias is seen in the L2 measurements.

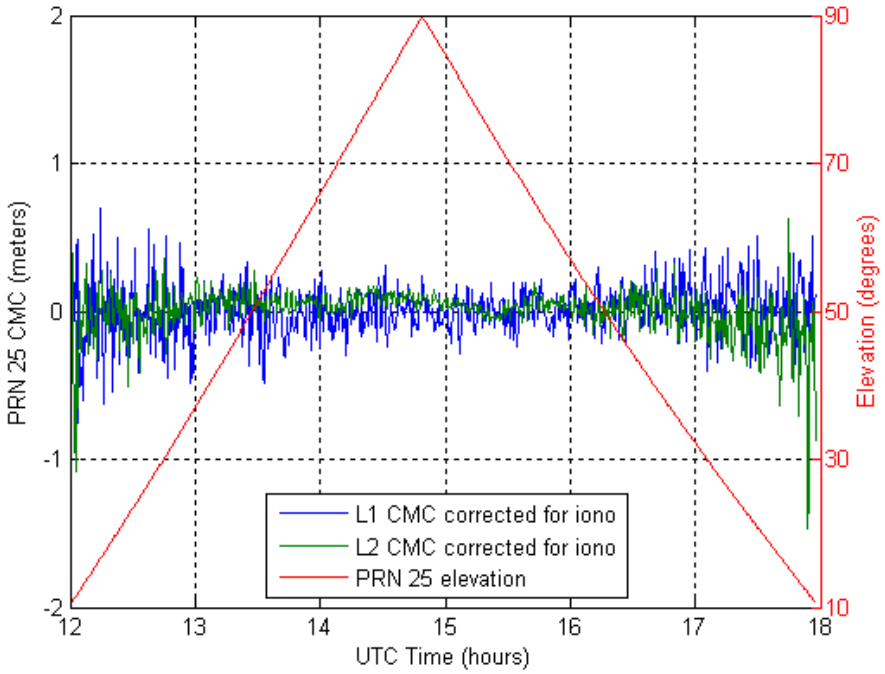

Figure 3. SVN 62 code-minus-carrier measurements after applying a dual-frequency ionosphere correction. The clock, orbit, troposphere, and ionosphere errors are all eliminated. No apparent elevation-dependent bias exists in either L1 or L2 measurements.

The elevation-angle effect was readily apparent on the measurements of SVN 49 received on June 19, 2010 and presented in Figure 2. (This bias was further verified by checking the data from other IGS sites and NSTB sites.) It shows the code/carrier difference for a single frequency after applying dual-frequency carrier-based ionosphere error corrections. Clock, orbit, troposphere, and ionosphere errors are all removed. The figure indicates that the SVN 49 anomaly is primarily in the L1 band; the code-minus-carrier (CMC) with ionosphere correction for PRN 1 has a bias highly correlated with the satellite elevation. The bias has a relative shift of 1.5 meters from a low elevation of 15° to a high elevation of 77°. The L2 CMC curve is flatter, although there appears to be a bias of about 0.4m in the opposite direction.

Figure 3 shows a similar plot for the L1 signal on SVN 62. The plot reveals there is no noticeable dependence on elevation angle from a low elevation of 10° to a high elevation of 89°.

SBAS and GBAS Models for Signal Deformation

Assuming no internal reflections or elevation angle dependencies, SBAS and GBAS generally classify potential signal deformations into two types: digital and analog. Digital distortions

occur when timing of the individual chip transitions of the transmitted codes vary from ideal. They are modeled as either an advance or delay of the rising or falling edge of a C/A code chip and can create "dead zones" (i.e., plateaus) atop an ideal correlation peak. (See figures 3 and 4 below.) The following sections compare both types of nominal deformations for the SVN 62 to those measured for the legacy constellation of satellites.

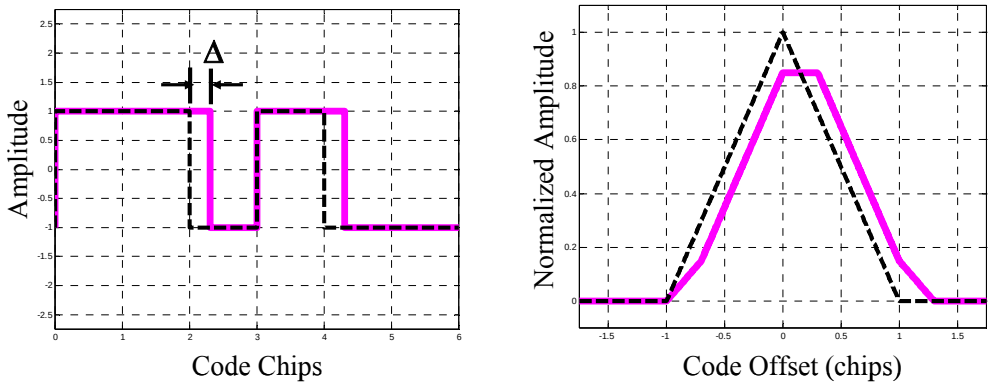

Figures 3 and 4. Example of digital code distortion model and its effect on the correlation peak

Analog deformations result from filter limitations in either the signal transmission path or the receiver hardware. Theses create oscillations that causer the correlation peak to become asymmetric. This is illustrated by Figures 5 and 6 below.

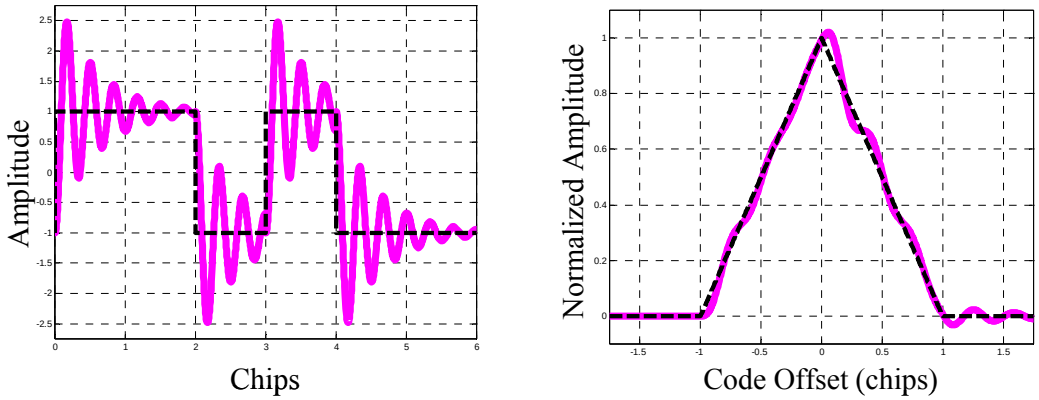

Figures 5 and 6. Example of analog code distortion model and its effect on the correlation peak

To characterize either type of distortion requires high-gain, high-resolution measurements of the transmitted signals. The basic technique for measuring digital code distortions is to compute successive differences between the ideal code chip width and the measured ones for each PRN. (A more complete discussion of these techniques and a completed summary of digital distortions will presented by Gabriel Wong at the September ION GNSS-2010 conference in Portland, Oregon.)

The first measurement of this type was published in 2004. Figure 7 summarizes that work by plotting digital distortion results for L1 C/A code as a function of GPS space vehicle numbers (SVN) shown in chronological order of launch date. That study revealed that the largest distortions were observed on the Block IIR satellites.

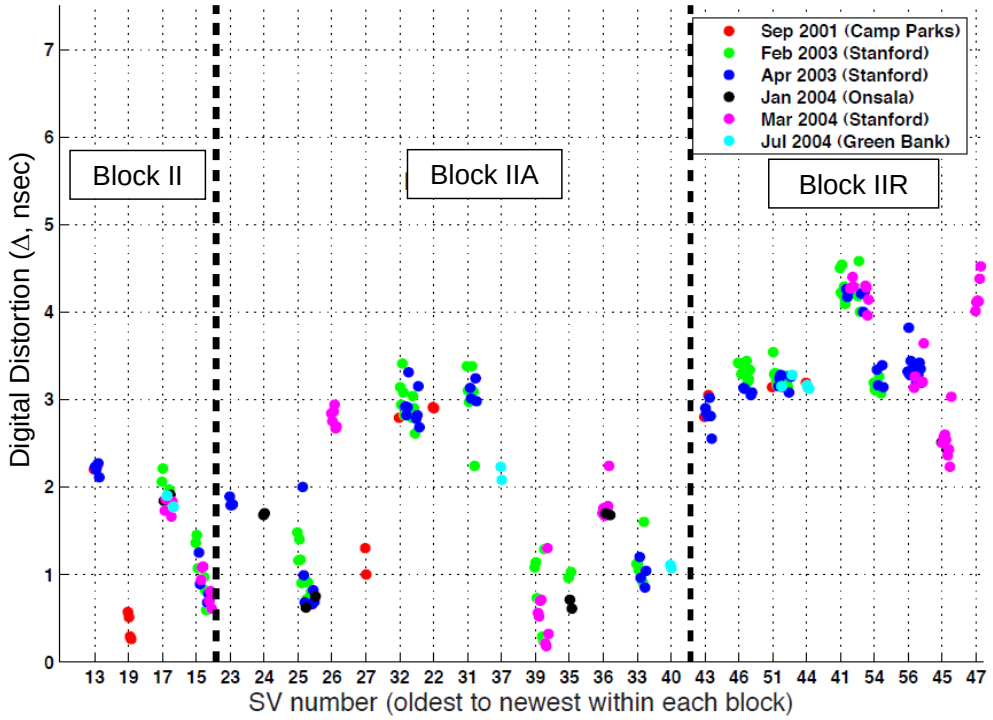

Figure 7. Historical digital distortion summary plotted as a function of SVN (from earliest to latest launch date). (Mitelman, A. *Signal quality monitoring for GPS augmentation systems*, Ph.D Dissertation, Stanford University, December 2004)

Figure 8 provides more recent estimates for digital distortion for L1 C/A code on 17 SVs using data taken from between 2008 and 2010. It is fairly consistent with the previous findings; it reveals that the Block IIR satellites continue to possess the largest amount of digital distortion. The Block II-RM SVs, however tend to have much smaller digital distortion.

The digital distortion on the SVN 62 L1 C/A code is comparable to that of the Block IIR-M satellites. Both have digital distortion estimates on the order of 1-1.5ns. The distortion for the L5 signal is significantly larger however. It is approximately 6ns for the in-phase code component and slightly more than 4ns for the quadrature component. (The standard deviation for each of these measurements was approximately 0.25ns for the Block IIA and IIR satellites but was slightly higher for the Block IIR-M and IIF SVs.) It is somewhat unexpected that the digital distortion estimates differ so much for different signals on the same satellite.

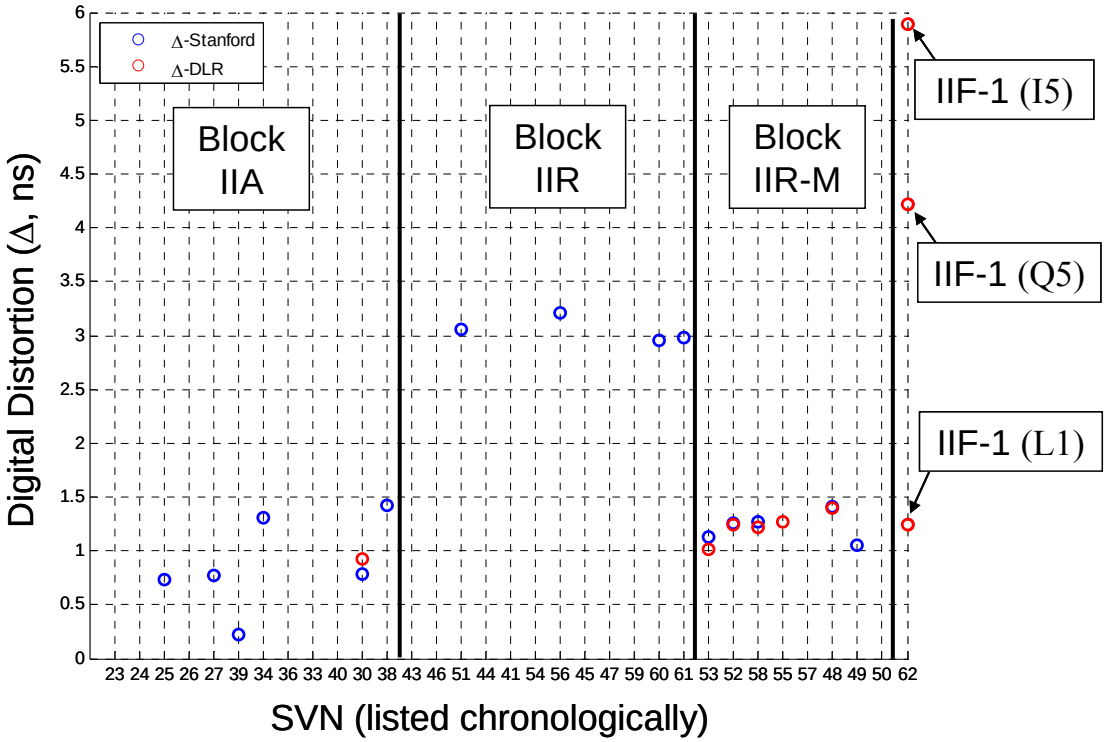

Figure 8. Recent digital distortion summary plotted as a function of SVN (from earliest to latest launch date). This uses data taken between June 2008 and 2010. Three results appear for SVN 62: One for L1 C/A code, one for I5 (L5, In-phase) and Q5 (L5, quadrature).

Figure 9 compares the C/A code chip shapes, or step-responses, for the GPS SVs represented in Figure 8. It can be seen that all the responses for all the SVs are fairly similar. Each has an overshoot ranging from about 110% to about 120% of the steady-stare amplitude, and the overshoot for SVN62 lies approximately in the middle of this range. (The maximum overshoot corresponds to SVN56, and the minimum corresponds to SVN58.) The step response for SVN62 does, however, seem to be more damped. Its settling time appears significantly smaller than for the other responses.

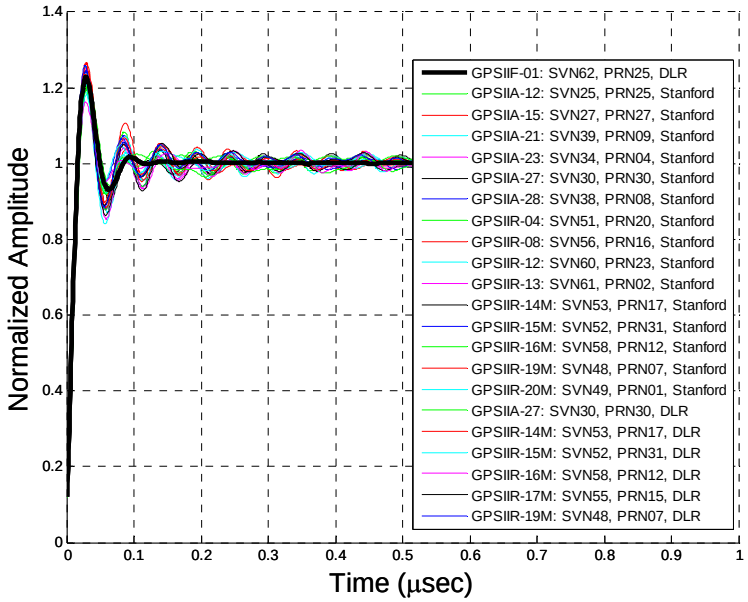

Figure 9. Comparison of the step responses on the L1 C/A codes 17 of GPS satellites. (The response of SVN62 is depicted by the heavy black trace.)

Figure 10 compares the step responses of L1 C/A and the two L5 codes of SVN 62. In order to better compare the effects of the filter after transition, segments of the L5 code that had five positive chips in row were selected for display in the figure. Thus, what is shown is five times longer than a single L5 chip width. As expected, the two L5 signals agree quite closely with each other. Ideally, these would be identical since all the signals pass through the same filtering components on the satellite. However, some small differences can be seen. Measurement error may account for some of the differences observed. The L1 C/A signal shape is quite similar to the L5 response, which indicates similar filter designs in the two different frequency paths.

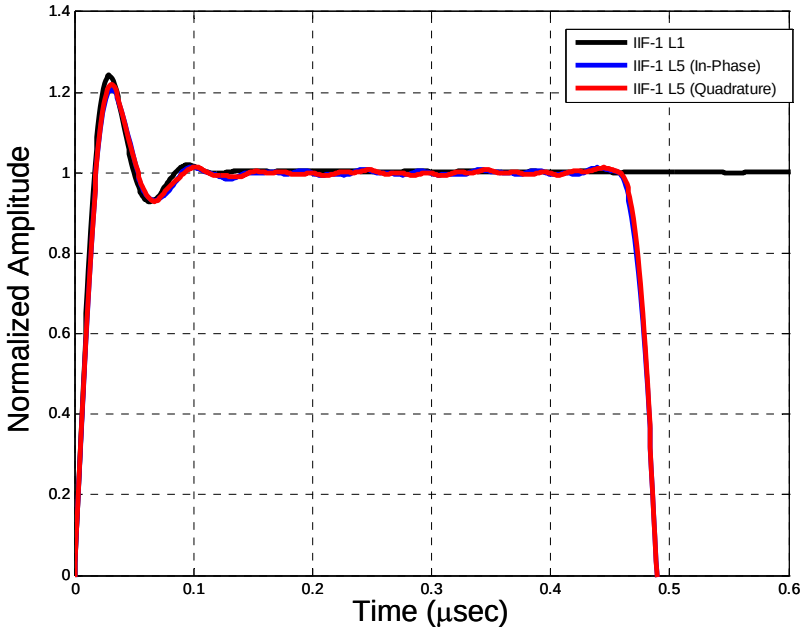

Figure 10. Comparison of the step responses on three codes transmitted from SVN 62: L1 C/A (black), L5 In-phase and Quadrature (Blue and Red, respectively).

Range Errors Due to Signal Deformations

If only digital distortion were present, the range errors would be relatively small. For example, Figure 11 shows the results for $-10 \leq \Delta \leq 10$ns on L1 C/A code assuming all WAAS users have early-minus-late (EML) discriminators. For the SVs discussed in this article, the largest range error due to nominal digital distortion alone would be less than 1cm. For SVN 62, it would be less than 2mm.

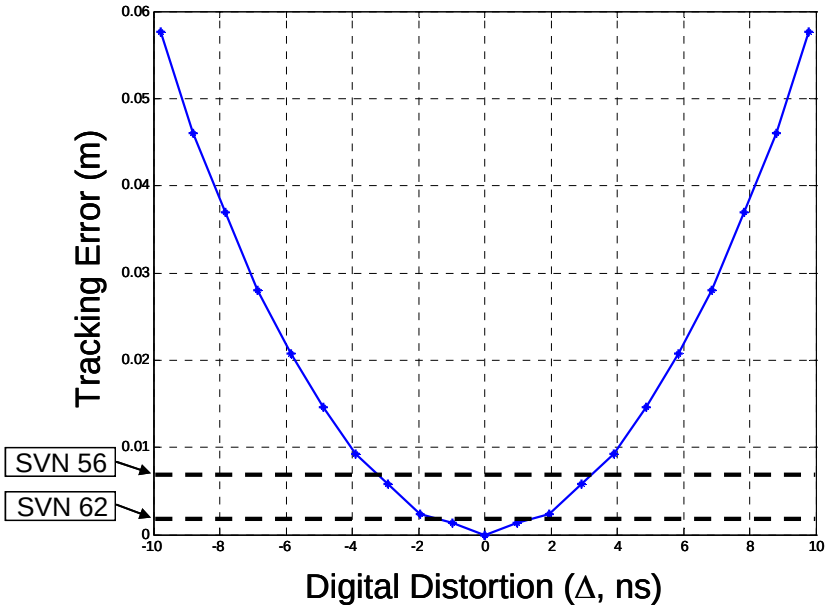

Figure 11. Modeled WAAS user tracking errors on L1 C/A code due to digital distortion only. Errors have been differentially corrected by the WAAS reference station receiver (Early-minus-late discriminator at 0.1-chip spacing and a filter having 18MHz bandwidth). User receiver properties are modeled according to the constraints defined in the Minimum Operational Performance Standards (MOPS) DO-229D.

This simplified analysis does not account for the analog distortion effects observed in Figures 9 and 10 however. It also does not account for the fact that true range errors result from tracking error differences between the actual satellites signals—which are never completely ideal. For an actual set of range sources, the analog and digital distortions combine. They both deform the correlation peak. A receiver subsequently processes and estimates tracking errors on these distorted peaks. The range error due to signal deformations is determined by the tracking error on any individual signal made relative to the others.

The relative nominal signal deformation performance for all satellites can be found by forming correlation peaks from the measured codes from different SVs, estimating the early-minus-late (EML) tracking errors across a range of correlator spacings (referenced to a single spacing), and then comparing these estimates to each other. Ideal, perfectly symmetry peaks would produce results that are independent of correlator spacing. Actual signals, however, will produce estimates that vary with correlator spacing. Signal deformation is what causes these variations to differ from satellite-to-satellite.

Figure 12 computes relative tracking errors for the previously discussed SVs assuming early-minus-late (EML) tracking and wide bandwidths (>30 MHz). Because variations that are common across all satellites do not create a differential error, an average, common-mode distortion effect has been removed. The reference correlator spacing assumed here is 0.1-chip (~100ns), consistent with the current WAAS reference receiver configuration. Since no additional filtering or receiver processing applied here, all the traces have zero relative error by definition at that spacing.

Given a 100ns reference correlator spacing, the largest range errors due to signal deformation may occur for users who have wider correlator spacings. This is consistent across all the satellites—including SVN 62. The trace corresponding to SNV 62, while not in the middle, is not at either extreme in this grouping. At the narrowest spacing (~50ns), the worst case difference in range error (i.e., maximum error – minimum error) over all traces is approximately 50cm. The range error is about 10cm for SVN 62 at this spacing. The largest differences occur at around 200ns, where the worst difference in range error approaches 1.6m. The range error for SVN 62 is about 0.55m at that offset. These results indicate that the L1 C/A code on SVN 62 conforms to the deformation status of the existing constellation and likely introduces minimal additional nominal deformation biases of concern.

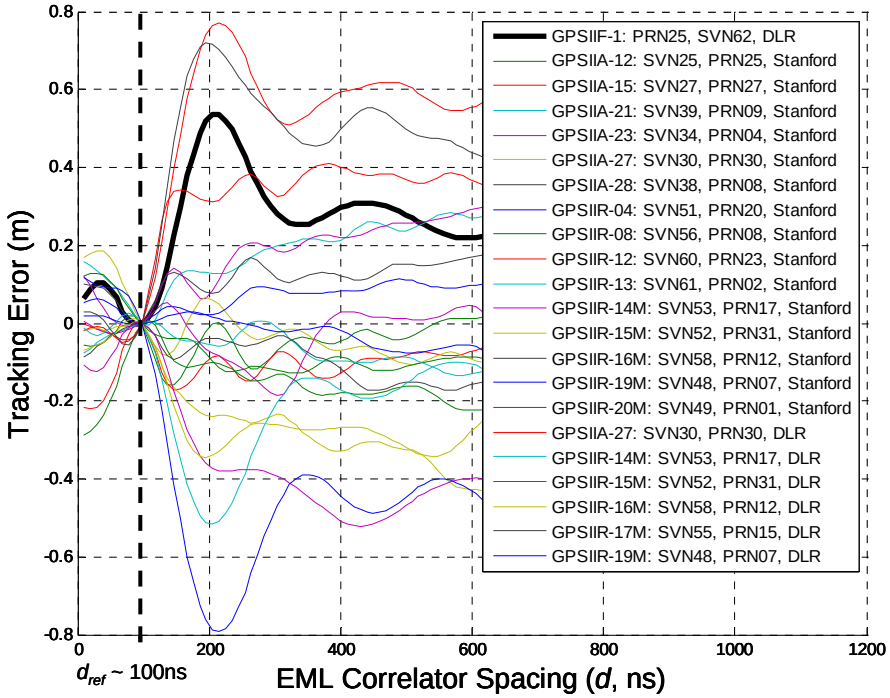

Figure 12. Tracking errors of all satellites relative to mean across all satellites plotted as a function of Early-Minus-Late (EML) correlator spacing, *d*.

Conclusions

The L1 C/A code on SVN 62 appears to meet or exceed expectations with respect to signal deformations. No noticeable elevation angle dependence can be observed. With an estimated digital distortion of only ~1.25ns, it appears to be among the highest quality signals in terms of digital distortion on L1 C/A. This signal also seems nearly prototypical in terms of nominal analog distortion since its transient effects (i.e., overshoot, rise time, peak time, and settling time) are essentially at the center of the others. In fact, its analog step response seems superior in that the transients damp out more quickly than observed in the other satellites. The relative range errors, too, appear to be within the bounds established by the other satellites measured thus far. All these factors indicate that the L1 C/A code on SVN 62 is a good signal that is suitable for use

by aviation. More specifically, SBAS and GBAS should be able to seamlessly incorporate this new satellite using their existing monitors and assumptions.

The L5 codes are more difficult to conclusively assess for aviation. As this is the first true GPS L5 signal, there are currently no existing SBAS or GBAS L5 signal deformation monitors; relatively few assumptions have been made about them. Certainly larger digital distortions were observed on the L5 codes, but this does not necessarily imply the signal is anomalous. The analog distortion on L5 corresponds well with those observed on the L1 C/A code, but this alone does not imply the signal is well-behaved. Each of these results needs to be compared to other GPS L5 signals to make a true assessment of the quality of any individual signal.

It should be further noted that at the time of writing of this paper, the broadcasts from this satellite had only recently been initiated. Testing of the signals was still being performed so these results may not represent the final operational configuration of the satellite. Still, this first look at the both the L1 and L5 navigation signals from this satellite cause us to be optimistic about the future of the GPS constellation and dual-frequency operations for aviation users.

Hardware Description

Many of the high-gain measurements used for the analyses discussed herein were taken using the 46-meter parabolic dish antenna at Stanford University and operated by Stanford Research Institute. The antenna achieves a 45dB gain and also incorporates a 50dB low-noise amplifier ($T_{eq} \approx 40K$). It has a 50MHz bandwidth over the L-band. (See Figure 4.) This is the same antenna that was used to take the code distortions measurements in Figures 7, 8, 9, 10 and 12. (The antenna and hardware used for the DLR measurements are described in the article entitled "On the Air: New Signals from the GPS IIF Satellite" in this issue of InsideGNSS.)

Acknowledgments

The authors gratefully acknowledge the support of the Federal Aviation Administration under CRDA 2000G028. This article contains the personal comments and beliefs of the authors and does not necessarily represent the opinion of any other person or organization.

Manufacturers

Stanford researchers use an Agilent 89640 Vector Signal Analyzer (VSA) from Agilent Technologies, Santa Clara California, USA. The data was processed by a software radio GNSS receiver. This receiver and the specialized signal authentication codebase are implemented in MATLAB from the MathWorks, Inc., Natick Massachusetts, USA.

Additional Resources

[1] Hegarty, C. J. and Chatre E., "Evolution of the Global Navigation Satellite System (GNSS)," in Proceedings of the IEEE Vol. 96, Issue 12, Dec. 2008.

[2] Minimum Operational Performance Standards (MOPS) for WAAS, DO-229D. *RTCA*

[3] Mitelman, A.M., (2005) *Signal Quality Monitoring For GPS Augmentation Systems,* Ph.D. Thesis, Stanford University, Stanford, CA.

[4] Spilker, J. J., Van Dierendonck, A. J., "Proposed New Civil GPS Signal at 1176.45 MHz," *Proceedings of the 12th International Technical Meeting of the Satellite Division of the Institute of Navigation* ION GPS-1999, September 1999.

Authors

R. Eric Phelts, Ph.D., is a research engineer in the Department of Aeronautics and Astronautics at Stanford University. He received his B.S. in Mechanical Engineering from Georgia Institute of Technology in 1995, and his M.S. and Ph.D. in Mechanical Engineering from Stanford University in 1997 and 2001, respectively. His research involves signal deformation monitoring techniques and analysis for SBAS, GBAS, and the GPS Evolutionary Architecture Study (GEAS).

Grace Xingxin Gao, Ph.D., is a research engineer in the GPS lab of Stanford University. She received the B.S. degree in mechanical engineering and the M.S. degree in electrical engineering, both at Tsinghua University, Beijing, China. She obtained the Ph.D. degree in electrical engineering at Stanford University. Her current research interests include GNSS signal and code structures, GNSS receiver architectures, and interference mitigation. She has received the Institute of Navigation (ION) Early Achievement Award.

Gabriel Wong is an Electrical Engineering Ph.D. candidate at the Stanford University GPS Research Laboratory. He has previously received an M.S.(EE) from Stanford University, and a B.S.(EECS) from UC Berkeley. His current research involves signal deformation monitoring for GNSS signals.

 **Liang Heng** is a Ph.D. candidate under the guidance of Professor Per Enge in the Electrical Engineering Department at Stanford University. He received the B.S. and M.S. degrees in electrical engineering from Tsinghua University, Beijing, China. His current research interests include GNSS signal processing and GPS modernization.

 **Todd Walter**, Ph.D., is a senior research engineer in the Department of Aeronautics and Astronautics at Stanford University. He received his Ph.D. from Stanford and is currently working on the Wide Area Augmentation System (WAAS), defining future architectures to provide aircraft guidance, and working with the FAA and GPS Wing on assuring integrity on GPS III. Key early contributions include prototype development proving the feasibility of WAAS, significant contribution to WAAS MOPS, and design of ionospheric algorithms for WAAS. He is a fellow of the Institute of Navigation.

 **Per Enge**, Ph.D., is a professor of aeronautics and astronautics at Stanford University, where he directs the GNSS Research Laboratory. He has been involved in the development of the Federal Aviation Administration's GPS Wide Area Augmentation System (WAAS) and Local Area Augmentation System (LAAS). Enge received his Ph.D. from the University of Illinois. He is a member of the National Academy of Engineering and a Fellow of the IEEE and the Institution of Navigation.

Stefan Erker
(TBD)

Steffen Thoelert
(TBD)